



Molecular Anti-Viral Drug Designing from *Hybanthus enneaspermus* - A Virtual Drug Screening

A.K. Ramya^{1*}, S. Poojasri², P. Annathai³, Muthupandian Saravanan^{4*}

- 1, 3 Research Associate, Golden jubilee Biotech Park for Women Society, Siruseri Village, Inside SIPCOT - IT Park, OMR, Navalur Post, Kanehipuram District - 603103, TamilNadu, India.
- 2 Department of Industrial Biotechnology, Bharath Institute of Higher Education and Research (BIHER), Selaiyur, Chennai - 600 073, TamilNadu, India.
- 4 Department of Microbiology and Immunology, Division of Biomedical Sciences, College of Health Sciences, Mekelle University, Mekelle 1871, Ethiopia.

ARTICLE HISTORY

Received: 07.01.2020

Accepted: 05.03.2020

Available online: 31.03.2020

Keywords:

Hybanthus enneaspermus, FT-IR, GC-MS, SARS-CoV-2, molecular drug design, in-silico anti-viral activity.

*Corresponding author:

Email : akramya@gmail.com¹
bioinfosaran@gmail.com

ABSTRACT

Study Background: *Hybanthus enneaspermus* medicinal plant are the natural reservoir of medicinal compounds to cure many diseases since the compounds have no adverse side effects. The current study focused on characterization of chemical compounds present and their in-silico anti-viral activity by adopting molecular drug designing method. Objective: SARS-CoV-2 outbreaks resulted approximately around one lakh deaths in all over the world. Still there is no particular drug for the viral infection treatment. To overcome and control this fatal infection, medicinal plants are the versatile solution with less side effects when compared to synthetic drugs. The Covid-19 spike protein, the key protein in viral transmission of host cells by membrane fusion mechanism. The main research of this work is to investigate the *Hybanthus enneaspermus* phyto-compounds by In-silico molecular drug designing approach against Covid-19 spike protein. Methodology: Molecular docking analysis of *Hybanthus enneaspermus* phytocompounds resulted from FT-IR and GC-MS analytical studies. The molecular drug designing softwares such as ACD ChemsSketch, AutoDock 4.2 version and 3D molecular visualization UCSF Chimera software were used. Results: Our study reports the phytochemical analysis of crude extract of *Hybanthus enneaspermus*. FT-IR, GC-MS revealed compounds were docked against SARS-CoV-2 proteins and lead compounds were summarized using MGL tool AutoDockvina 4.2 version. Docking results suggested that 3-Trifluoroacetoxypentadecane (-8.9), 9,12-Octadecadien-1-ol (-8.6), 9,12,15-Octadecatrienoic acid (-8.8), 9,12-Octadecadienoic acid (-9.2) had high binding affinity with minimum binding energies scoring function and hence considered as potential anti-viral inhibitory activity. Conclusion: Our molecular drug designing approach using *Hybanthus enneaspermus* data demonstrated that ability of designing of anti-viral drug against SARS-CoV-2. Moreover, this study suggested to perform in-vitro and in-vivo experiments to understand therapeutic effect much more better.

INTRODUCTION

Scientific review of *Hybanthus enneaspermus* In developing countries like India rely on herbal medicines to cure many health related problems due to

their no side effects and beneficial effects. Biologically, several plants were used to screen their phytocompounds to explore their medicinal properties [1-4]. The World Health Organization (WHO) suggested to use effective medicines plants to combat various health issues like anti-microbial, anti-oxidant, anti-

inflammatory and sedative effects due to their bioactive phytochemicals [5]. *Hybanthus enneaspermus* (Linn) F. Muell (Synonyms: *Ionidium suffruticosum*) belongs to *Violaceae* family is a perennial herb. Usually grow upto 60 cm height. This medicinal plant is used as diuretic, demulcent and tonic for mainly considered to men. Biologically, this plant was reported the presence of dipeptide alkaloids, aurantiamide acetate, beta sitosterol, sugars, flavonoids, tannins, catechins, phenols, anthraquinones, triterpenes, isocarborinol. Also, studies reported this plant have many bioactivity such as anticonvulsant, antidiabetic, antiplasmodial, antimicrobial [6] and anti-infertility [7]. Our main focus on this plant is to identify potent anti-viral activity phytochemical to target SARS-CoV-2 spike protein in order to combat their infection by following our traditional herbal medicine.

METHODOLOGY

Sample Preparation

Gram scale production was carried out from fine powder of whole plant from collected *Hybanthus enneaspermus*. 2000 grams of defatted crude sample was prepared by solvent extraction using petroleum ether at 60 ° to 80 ° temperature. The defatted crude sample was further subjected to methanol extraction at 38° for 72 hours in Soxhlet apparatus. After extraction, the solvents traces were removed by distillation under low pressure condition. The dried crude extract was done by vacuum drying process. Finally, the dried crude extract was weighed, labeled and stored at - 20 ° in deep freezer until further purposes.

FT - IR Analysis

Fourier Transform - Infrared spectroscopy analysis was performed for the identification of functional groups present in the crude extract of *Hybanthus enneaspermus*. The sample were scanned from 400 to 4000 cm^{-1} as the absorption radiation. The FT-IR analysis (Shimadzu - QP2010 PLUS, Japan) was performed by KBr pellet method and intensities of transmittance peaks were recorded and identification of functional groups present in dried powder of crude extract.

GC-MS Analysis

For GC-MS analytical study, solvent extracted and dried concentrated plant sample diluted in Carbinol was used. Furthermore, GC analysis was performed by setting parameters includes column oven temperature (50 ° with hold time 1 min), injection temperature (280 °), injection mode (split), pressure (49.5 kPa), total flow (8.7 mL/min), column flow (0.95 mL/min), ion source temperature (250 °), interface temperature (300 °). MS program includes start time (3 min), end time (39 min), ACQ mode (scan), scan speed (3333).

Molecular Drug Designing

Molecular drug designing strategy reduce the time, cost investment in development of new drugs from medicinal plants. In India, several medicinal plants have their own unique medicinal properties against various diseases. Folk medicines are still used by tribal culture of our India. To explore these medicinal compounds from plants includes both wet lab and dry lab methodologies. In our work, we extract crude from *Hybanthus enneaspermus* and analyzed their chemical composition by employing FT-IR and GC-MS analytical methods. The identified chemical compounds from the crude extract was used as a ligand to study SARS-CoV-2 proteins inhibition for combating

pandemic transmissions among human health. To achieve this, we perform molecular docking and molecular visualization softwares.

Compound Retrieval

The compounds for molecular drug designing was retrieved from the information of GC-MS analysis. From GC-MS analysis, we identified that crude extract have 23 compounds. Each compound structures were drawn using Chemsketch Software and converted it into PDB format by Open Babel Software. After then, the compounds were corrected for structure configuration and coordinates conformation by Steepest method energy minimization. Lastly, the prepared compounds were docking with different Covid-19 protein targets. The standard drugs Remdesivir and Hydroxychloroquine was considered as the positive reference index for inhibition activity.

Protein structure Preparation

Covid-19 targeted proteins amino acids sequence were retrieved from NCBI Database and modelled using Swiss Model web tool for docking [8-11]. The hetero atoms [HETATM] bound were not a part of the native protein was removed and energy minimized by steepest method. After that, the optimized protein targets were checked for molecular docking to identify a best anti-

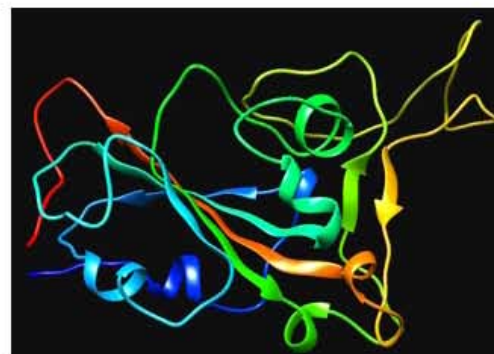


Fig. 1 : 3D modelled SAR-CoV-2 spike protein

viral activity.

Binding sites prediction

CASTp server was used to predict active residues of SARS-CoV-2 spike glycoprotein macromolecule [12]. The active site residues were used to identify X, Y and Z grid coordinates during molecular docking.

Molecular Docking

The Molecular drug docking was performed by AutoDockvina 4.2 version software. The prepared macromolecule were opened in a AutoDockvina 4.2 virtual screening tool by load molecule and edited by adding polar hydrogen bonds, water molecules were deleted and converted macromolecule into pdbqt format. The pdbqt format is a simplest version that add necessary hydrogen atoms in a macromolecule. Next, the prepared ligands were imported, checked for root detecting and then converted into AutoDockvina ligand pdbqt format for comfort docking. AutoDockvina dock ligands with macromolecule in a 8 different scoring configuration functions for the best ligands fitting and accuracy of binding affinity. The lowest minimum binding energy with a macromolecule showed high binding affinity and aided in drug development processes to

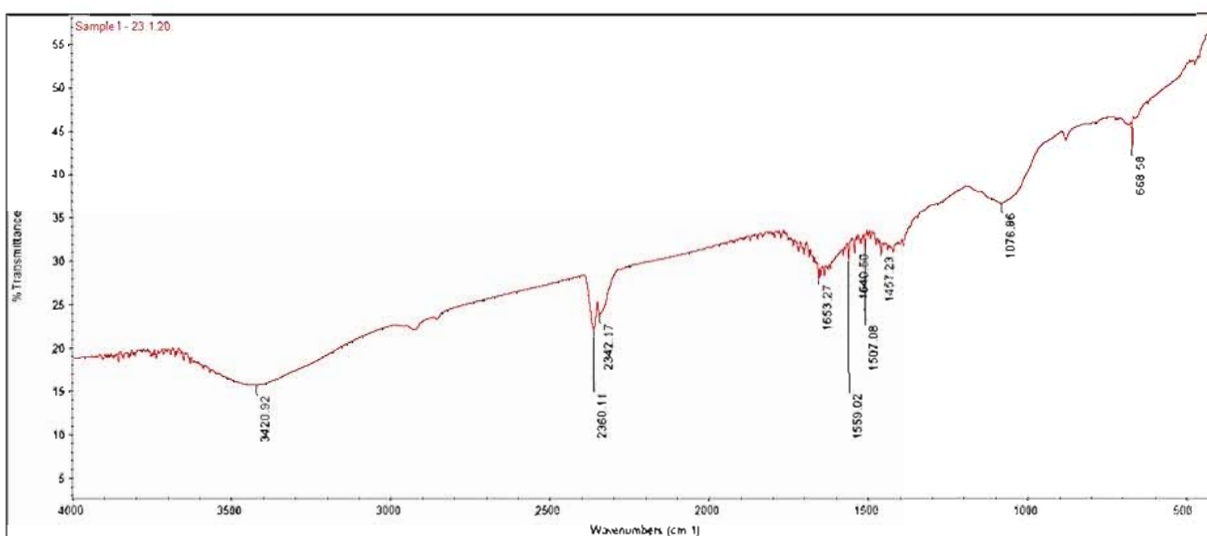


Fig. 2 : From the FT-IR analysis of *Hybanthus enneaspermus* showed peaks at both group frequency region (1500 - 4000 cm^{-1}) and fingerprinting region (400 - 1500 cm^{-1}) of IR spectra. The FT-IR spectra of silver nanoparticles showed various prominent peaks at 3420.92, 2360.11, 2342.17, 1653.27, 1559.02, 1540.50, 1457.23, 1507.08, 1076.86, 668.58. [Table No.1] conformed the presence of functional groups such as secondary amine, primary amine, nitro compounds, aromatics, organophosphorus, fluoroalkanes, chloroalkanes.

Table 1 : Peaks values at two important regions of IR spectra.

Functional Group Region or Group Frequency Region	Fingerprinting Region
3420.92 cm^{-1}	1457.23 cm^{-1}
2360.11 cm^{-1}	1076.86 cm^{-1}
2342.17 cm^{-1}	668.58 cm^{-1}
1653.27 cm^{-1}	
1559.02 cm^{-1}	
1540.50 cm^{-1}	
1507.08 cm^{-1}	

Table 2 : Functional Group Region Frequencies (1500 - 4000 cm^{-1})

IR Spectrum- Wavenumber (cm^{-1})	Molecular Motion (Chemical Bond type)	Functional Groups
3420.92 cm^{-1}	secondary amine, amide	N-H
2360.11 cm^{-1}	Overtone	-
2342.17 cm^{-1}	Overtone	-
1653.27 cm^{-1}	Amides	C=O
1559.02 cm^{-1}	Primary amines	N-H
1540.50 cm^{-1}	Nitro compounds	N-O
1507.08 cm^{-1}	Aromatic	C=C

avoid failures in later. The best poses of docked macromolecule were analyzed for amino acids interactions between ligands, hydrogen bond formation and interaction chains using UCSF Chimera 3D molecular visualization tool.

ADMET Data Prediction

Absorption, Distribution, Metabolism, Excretion and Toxicity (ADMET) properties plays an versatile part in drug designing steps. These properties accounted for the major reason in drug failure in clinical trial phases. In traditional drug development process, the ADMET properties were employed at the lateral phase of drug development process. Due to drug failure reasons, nowadays ADMET calculations were made initially before synthesizing the drug molecules in order to avoid poor bioactive drug molecules and other R&D development costs. All ADMET predictions were made by using Swiss ADME and

ProTox-II, a web-based application for predicting ADME data and building drug-like library using in-silico method [13,14].

RESULTS

GCMS data analysis

After GC-MS analysis, the obtained spectrum was observed and tabulate it to investigate their in-silico medicinal property. The observed spectrum revealed that there is a present of 24 compounds and evaluated their in-silico anti-viral activity.

Minimum Binding energy summary

Molecular docking results revealed most lowest minimum binding energy docked with SARS-CoV-2 spike protein. Further, the lead compounds were analyzed for intramolecular interactions such as hydrogen bonds formation, hydrophobic interaction and π -interaction which are pivotal to protein-ligand

Table 3 : Fingerprinting Region Frequencies (1500 - 4000 cm^{-1})

Fingerprinting Regions	Molecular Motion (Chemical Bond type)	Functional Groups
1457.23 cm^{-1}	Organophosphorus compound	P-C
1076.86 cm^{-1}	Fluoroalkanes	C-X
668.58 cm^{-1}	Chloroalkanes	C-X

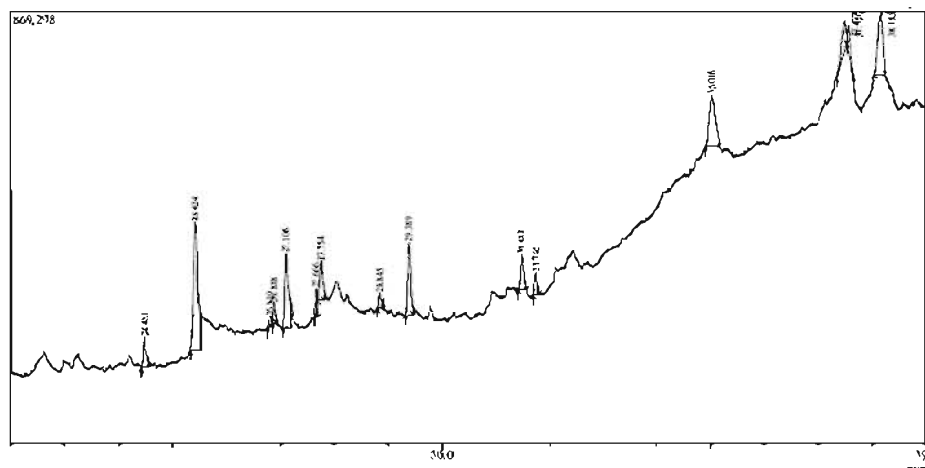
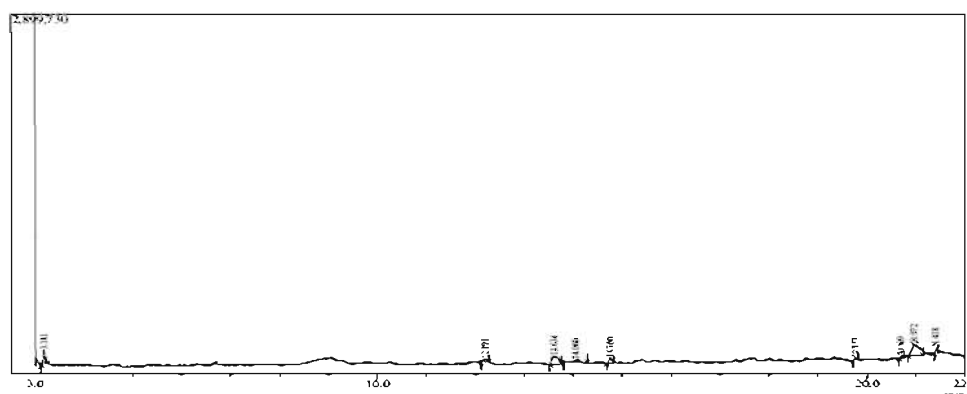
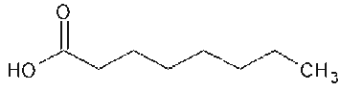
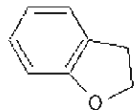

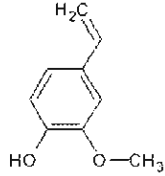

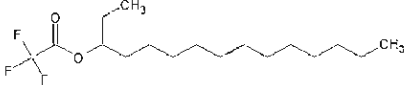
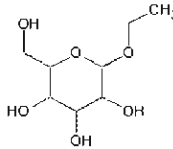

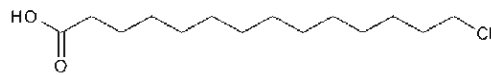
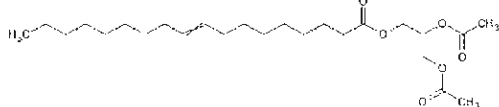
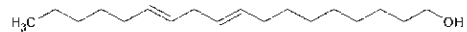
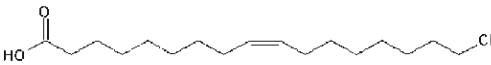
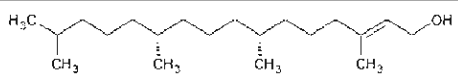


Table 3 : FGC-MS peaks of *Hybanthus enneaspermus* were interpreted by comparing the reference of National Institute Standard and Technology (NIST) library and Wiley library.

Table 4 : Phyto-Compounds summary

S. No.	Phytocompounds	Molecular structure
1.	Octanoic acid	
2.	2,3-dihydro-benzofuran	
3.	Nonanoic acid	
4.	2-Methoxy-4-vinylphenol	
5.	Tetradecanal	
6.	3-Trifluoroacetoxypentadecane	
7.	Ethyl-alpha.-d-glucopyranoside	
8.	Hexadecanal	
9.	Pentadecanoic acid	
10.	9-Octadecenoic acid	
11.	9,12-Octadecadien-1-ol	
12.	9-Octadecenoic acid (Oleic acid)	
13.	Phytol (2-Hexadecen-1-ol)	



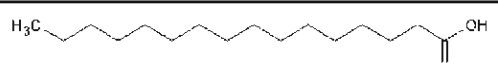
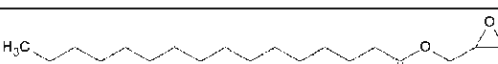


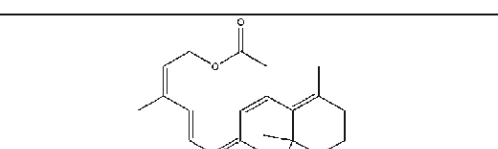
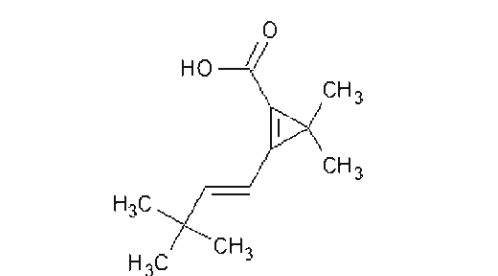
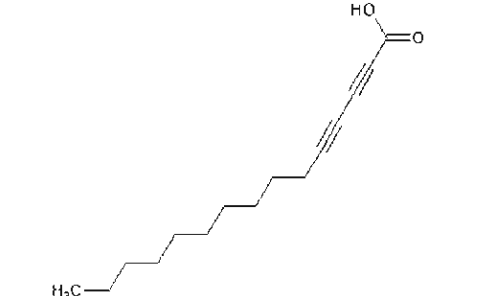
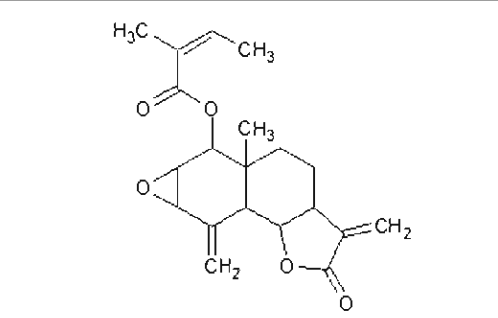
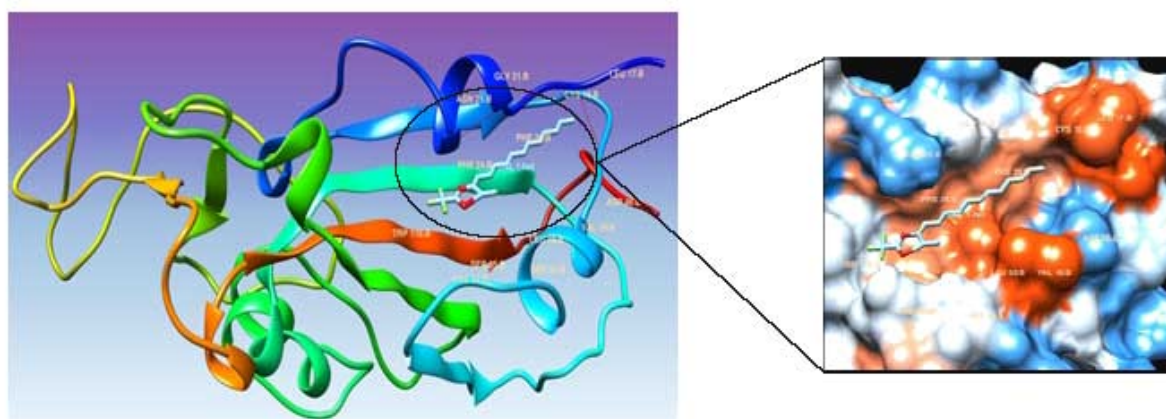
14.	9,12,15-Octadecatrienoic acid	
15.	9,12-Octadecadienoic acid	
16.	Hexadecanoic acid	
17.	Glycidylpalmitate	
18.	13-Octadecenal	
19.	Octadecanoic acid	
20.	Retinol	
21.	2-(3,3-Dimethyl-1-Butynyl)- 3,3-Dimethyl-1-Cyclopropene-1	
22.	2,4-Pentadecadiynoic acid	
23.	5A-Methyl-3,8-Dimethylene- 2- oxod	

Table 5 : Minimum binding energy result summary

S.No.	Phytocompounds	Minimum Binding Energy
1)	Octanoic acid	- 4.0
2)	2,3-dihydro-benzofuran	- 5.0
3)	Nonanoic acid	- 4.5
4)	2-Methoxy-4-vinylphenol	- 4.9
5)	Tetradecanal	- 5.5
6)	3-Trifluoroacetoxypentadecane	- 8.9
7)	Ethyl- α -D-glucopyranoside	- 5.8
8)	Hexadecanal	- 5.3
9)	Pentadecanoic acid	- 4.93
10)	9-Octadecenoic acid	- 4.1
11)	9,12-Octadecadien-1-ol	- 8.6
12)	9-Octadecenoic acid (Oleic acid)	- 5.33
13)	Phytol (2-Hexadecen-1-ol)	- 5.6
14)	9,12,15-Octadecatrienoic acid	- 8.8
15)	9,12-Octadecadienoic acid	- 9.2
16)	Hexadecanoic acid	- 4.8
17)	Glycidyl palmitate	- 8.0
18)	13-Octadecenal	- 8.4
19)	Octadecanoic acid	- 5.0
20)	Retinol	- 6.03
21)	2-(3,3-Dimethyl-1-Butynyl)-3,3-Dimethyl-1-Cyclopropene-1	- 3.6
22)	2,4-Pentadecadiynoic acid	- 4.26
23)	5A-Methyl-3,8-Dimethylene-2-oxod	- 5.9

**Fig. 4 : 3-Trifluoroacetoxypentadecane bound with SARS-CoV-2 spike protein with a binding affinity of - 8.9 kcal/mol**

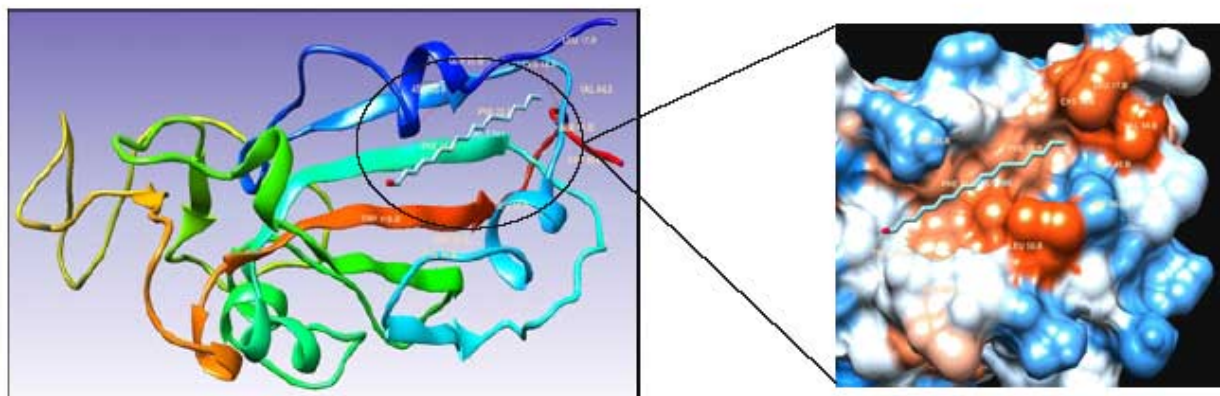


Fig. 5 : 9,12-Octadecadien-1-ol bound with SARS-CoV-2 spike protein with a binding affinity of - 8.6 kcal/mol

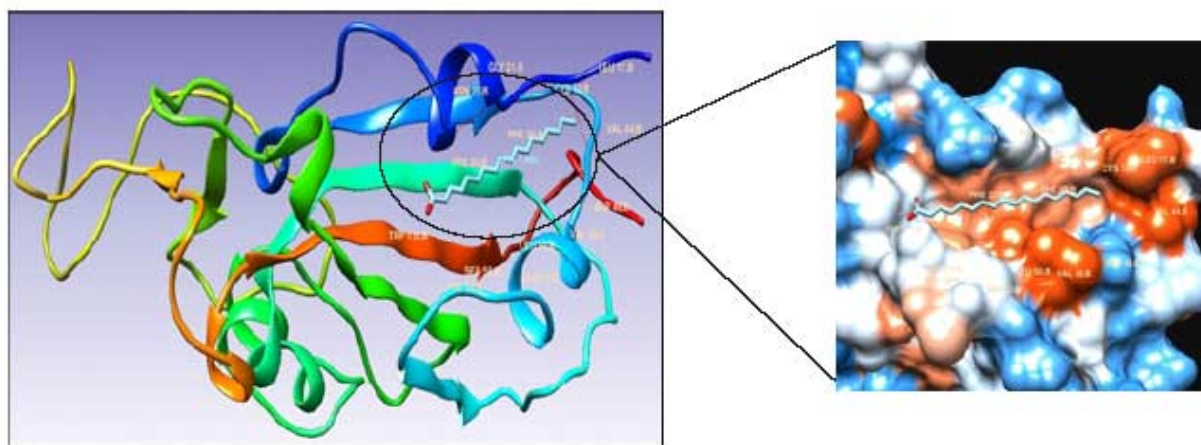


Fig. 6 : 9,12,15-Octadecatrienoic acid bound with SARS-CoV-2 spike protein with a binding affinity of - 8.8 kcal/mol

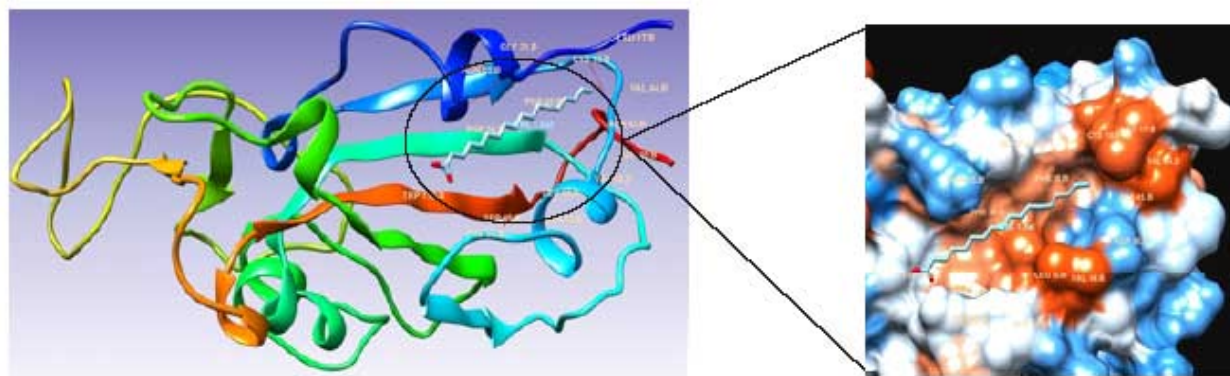


Fig. 7 : 9,12-Octadecadienoic acid bound with SARS-CoV-2 spike protein with a binding affinity of - 9.2 kcal/mol

recognition biological events. The summary of all docked compounds minimum binding energy were tabulated in [Table No.5].

Protein-ligand interaction analysis

Protein-ligand interactions are non-covalent bond interactions such as hydrogen bond formation, hydrophobic interactions and π -interactions and these have important functions in drug absorption, distribution, metabolism, excretion and toxicity

mechanisms. Protein-ligand interactions also involved in conformational changes to ensure high affinity states. Molecular recognition through protein-ligand interactions are fundamental parameters in molecular drug designing approach. To explain we identified amino acids involved in protein-ligand interactions and hydrogen bond formation by UCSF Chimera software. The best docked compounds were analyzed and found most of the bound ligands were interacted with (chain B) *TRP 118.B, PHE 24.B, SER 55.B, PHE 56.B, SER 53.B, LUE 50.B, VAL 49.B, ASP 46.B,*

LEU 17.B, CYS 18.B, PHE 20.B and formed hydrogen bonds between PHE 24.B HN-PHE 20.B O 1.986 Å, VAL 23.B HN-PHE 20.B O 2.271 Å, PHE 20.B HN-CYS 18.B O 1.915 Å, CYS 18.B HN-VAL 44.B O 1.783 Å.

Table 7 : ADMET properties prediction for 3-Trifluoroacetoxypentadecane

ADMET Properties of 3- Trifluoroacetoxypentade cane	Pharmacokinetics parameters	Values
	GI absorption	Low
	BBB permeant	No
	P-gp substrate	No
	CYP1A2 inhibitor	No
	CYP2C19 inhibitor	No
	CYP2C9 inhibitor	Yes
	CYP2D6 inhibitor	No
	CYP3A4 inhibitor	No
	Log K _p (skin permeation)	- 2.37 cm/s
	Bioavailability score	0.55
	Toxicity parameters	Values
	Toxicity class	Class 5
	LD50 mg/kg	3000 mg
	Hepatotoxicity probability	Inactive
	Carcinogenicity	Inactive
	Mutagenicity	Inactive
	Cytotoxicity	Inactive
	Immunotoxicity	Inactive

Table 8 : ADMET properties prediction for 9,12-Octadecadien-1-ol

ADMET Properties of 9,12-Octadecadien-1-ol	Pharmacokinetics parameters	Values
	GI absorption	High
	BBB permeant	No
	P-gp substrate	No
	CYP1A2 inhibitor	Yes
	CYP2C19 inhibitor	No
	CYP2C9 inhibitor	No
	CYP2D6 inhibitor	No
	CYP3A4 inhibitor	No
	Log K _p (skin permeation)	- 3.10 cm/s
	Bioavailability score	0.55
	Toxicity parameters	Values
	Toxicity class	Class 6
	LD50 mg/kg	10000 mg
	Hepatotoxicity probability	Inactive
	Carcinogenicity	Inactive
	Mutagenicity	Inactive
	Cytotoxicity	Inactive
	Immunotoxicity	Inactive

Table 9 : ADMET properties prediction for 9,12,15-Octadecatrienoic acid

ADMET Properties of 9,12,15-Octadecatrienoic acid	Pharmacokinetics parameters	Values
	GI absorption	High
	BBB permeant	Yes
	P-gp substrate	No
	CYP1A2 inhibitor	Yes
	CYP2C19 inhibitor	No
	CYP2C9 inhibitor	Yes
	CYP2D6 inhibitor	No
	CYP3A4 inhibitor	No
	Log K _p (skin permeation)	- 3.41 cm/s
	Bioavailability score	0.56
	Toxicity parameters	Values
	Toxicity class	6
	LD50 mg/kg	10000 mg
	Hepatotoxicity	Inactive
	Carcinogenicity	Inactive
	Mutagenicity	Inactive
	Cytotoxicity	Inactive
	Immunotoxicity	Inactive

Table 10 : ADMET properties prediction for 9,12-Octadecadienoic acid

ADMET Properties of 9,12-Octadecadienoic acid	Pharmacokinetics parameters	Values
	GI absorption	High
	BBB permeant	Yes
	P-gp substrate	No
	CYP1A2 inhibitor	Yes
	CYP2C19 inhibitor	No
	CYP2C9 inhibitor	Yes
	CYP2D6 inhibitor	No
	CYP3A4 inhibitor	No
	Log K _p (skin permeation)	- 3.05 cm/s
	Bioavailability score	0.56
	Toxicity parameters	Values
	Toxicity class	Class 6
	LD50 mg/kg	10000 mg
	Hepatotoxicity	Inactive
	Carcinogenicity	Inactive
	Mutagenicity	Inactive
	Cytotoxicity	Inactive
	Immunotoxicity	Inactive

ADMET analysis

Discussions

Many number of fatty acids were tested against enveloped viruses and non-enveloped viruses to study its antiviral activity. Based on the results short-chain and long-chain saturated fatty acids had no effects on antiviral activity. Medium-chain saturated and long-chain unsaturated fatty acids had high activity against enveloped viruses. Antiviral fatty acids cause leakage, disintegration of envelope proteins and virus particles of enveloped viruses [15].

Many naturally available fats and dietary oils are the major source of fatty acids and have efficient anti-microbial activities [16]. The pharmacological composition of many plants are not yet explored. Our present work demonstrated the identification of *H. lenneuspermus* phytochemicals and their in-silico antiviral activity against SARS-CoV-2 spike protein. From molecular docking study, we found 9,12,15-Octadecatrienoic acid, 9,12-Octadecadienoic acid, 13-Octadecenal compounds have

inhibitory action against our 3D modelled SARS-CoV-2 spike protein.

3-Trifluoroacetoxypentadecane - A chemical structure contains a total of 52 bonds which includes 21 non-hydrogen bonds, 1 multiple bonds, 1 double bond, 1 ester and 14 rotatable bonds.

9,12-Octadecadien-1-ol - also called linoleyl alcohol or fatty alcohol produced by reduction reaction of linoleic acid. Fatty alcohols are long chain alcohols naturally derived from plants waxes. Fatty alcohols have been reported as plasma cholesterol lowering ability in humans.

9,12,15-Octadecatrienoic acid - Linolenic acid is one of an essential fatty acid belongs to the class of omega-3-fatty acids. It is commonly found in plants in high concentration and also reported inhibition of prostaglandin synthesis there by reducing inflammation and prevents some chronic diseases. Since, linolenic acid is not synthesized by mammals and majorly depends on plants rich in linolenic acid. When it is incorporated

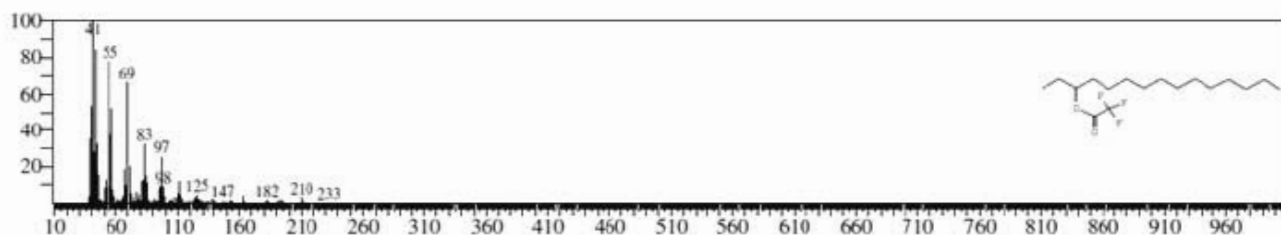


Fig. 7 : GC-MS peak of 3-Trifluoroacetoxypentadecane

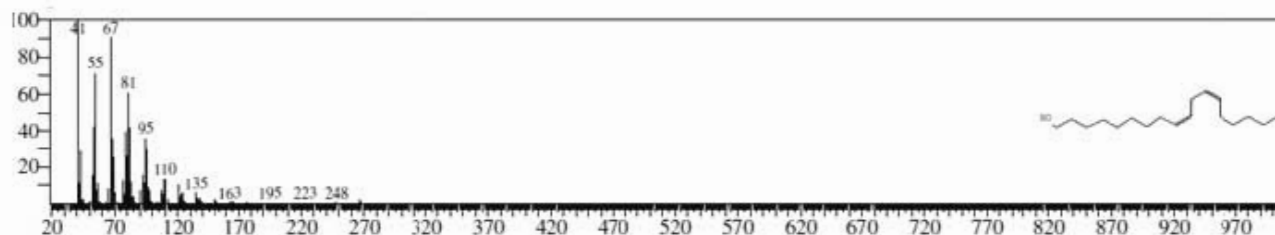


Fig. 8 : GC-MS peak of 9,12-Octadecadien-1-ol.

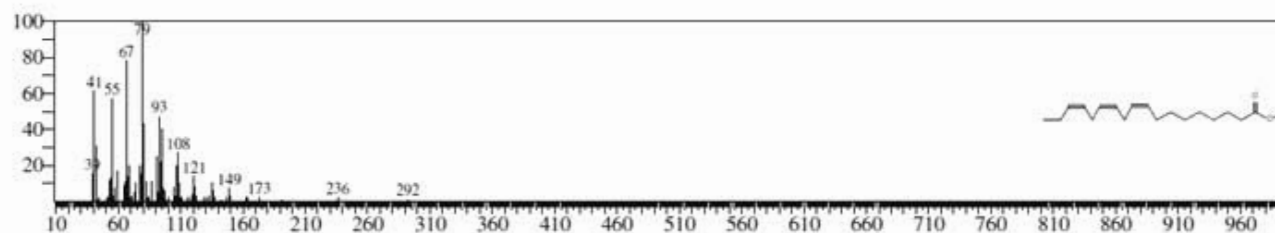


Fig. 9 : GC-MS peak of 9,12,15-Octadecatrienoic acid.

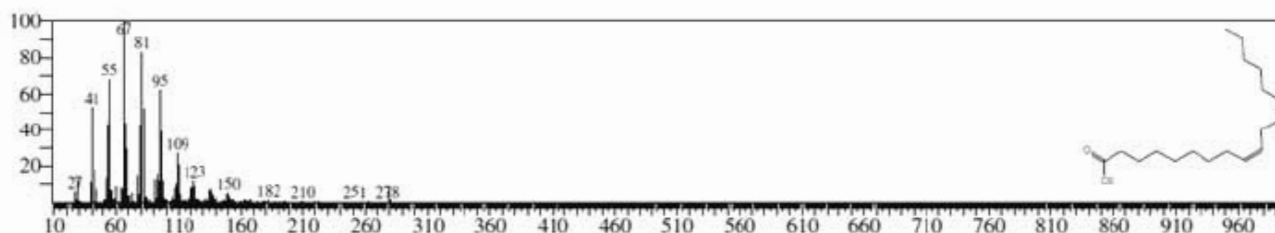


Fig. 10 : GC-MS peak of 9,12-Octadecadienoic acid.

into the plasmamembrane (phospholipids bilayer), they changes the cell membrane dynamic properties such as permeability, fluidity, flexibility and disruption on membrane bound enzymes or proteins [17].

9,12-Octadecadienoic acid -Linoelaidic acid is derivative of linoleic acid fatty acid and majorly studied in men due to their cancer modulating ability, obesity function, immunological functions, atherosclerosis and diabetic conditions. This fatty acids was prepared by hydrogenation reaction of plant oils by industrial scale [18].

CONCLUSION

Hybanthus enneaspermus a medicinal plant which have various bioactive properties. In this present work, we attempt to identify phytochemicals by FT-IR and GC-MS analysis revealed 24 phytochemicals presence in the crude extract of *H. enneaspermus*. GC-MS analysis demonstrated that the plant crude extract was rich in fatty acids. We carried molecular docking study to explore the identified phytochemicals bioactivity characteristics and found it has in-silico inhibitory activity against SARS-CoV-2 spike protein. Thus our study contributed to find a bioactive compounds that having anti-viral activity to combat SARS-CoV-2 pandemic infection.

These results explained naturally occurring plant derived fatty acids have antiviral activity. Therefore, fatty acids have antiviral response against SARS-CoV-2 spike protein and our investigative study recommended to take dietary fatty acids for Covid-19 infected patients to combat the disease aggressiveness.

Area of Conflict

All the authors declares no area of conflict

ACKNOWLEDGEMENT

I acknowledged Nanotechnology Research Centre (NRC), SRMIST for providing the research facilities for GC-MS analysis and FT-IR analysis.

REFERENCES

1. Waller DP. Methods in ethnopharmacology. J Ethnopharmacol 1993; 38: 189-195.
2. Perumal-Samy R, Patricraja D. Antibacterial activity of aqueous extracts of some selected weeds. Acta Bot India 1996; 24: 113-114.
3. Gajalakshmi S, Vijayalakshmi S, Devi Rajeswari V. Phytochemical and pharmacological properties of *Annona Muricata*: A Review. Int J Pharm Pharmaceut Sci 2012; 4(2): 3-6.
4. Dhabhai K, Bhargav S, Batra A. In vitro & in vivo antibacterial comparative study on *Acacia Nilotica* L. Int J Pharm PharmaceutSci 2012; 4(1): 174-175.
5. Keshari RB., et al. "Mental health challenges and possible solutions with special reference to anxiety". *International Research Journal of Pharmacy* 2.9 2011;37-42.
6. D.K.Patel R. Kumar K.Sairam S.Hemalatha. *Hybanthus enneaspermus* (L.) F. Muell: a concise report on its phytopharmacological aspects. *Chinese Journal of Natural Medicines* 2013; 11(3):199-206.
7. Nathiya S, and SenthamilSelvi R, Anti-infertility of *Hybanthus enneaspermus* on endosulfan induced toxicity in

- male rats, *International Journal of Medicine and Biosciences*, IJMB 2013;2(1): 28-32.
8. Guex N., Peitsch, MC, & Schwede T. Automated comparative protein structure modeling with SWISS-MODEL and Swiss-PdbViewer: a historical perspective. *Electrophoresis* 2009;30 (1):162-73.
9. Schwede T, Kopp J, Guex N and Peitsch MC. SWISS-MODEL: an automated protein homology-modeling server. *Nucleic Acids Research* 2003;31:3381-3385
10. Guex N, Diemand A and Peitsch MC. Protein modelling for all. *TiBS* 1999;24:364-367.
11. Mishra P, Günther S. New insights into the structural dynamics of the kinase JNK3. *Sci Rep.* 2018;8(1):9435.
12. Tian et al., *Nucleic Acids Res.* 2018. PMID: 29860391 DOI: 10.1093/nar/gky473.
13. The main article describing the web service and its underlying methodologies is Swiss ADME: a free web tool to evaluate pharmacokinetics, drug-likeness and medicinal chemistry friendliness of small molecules. *Sci. Rep.* 2017;7:42717.
14. Banerjee P., Eckert O.A., Schrey A.K., Preissner R.: ProTox-II: a webserver for the prediction of toxicity of chemicals.
15. Thormar H, Isaacs CE, Brown HR, Barshatzky MR, Pessolano T. Inactivation of enveloped viruses and killing of cells by fatty acids and monoglycerides. *Antimicrob Agents Chemother.* 1987;31(1):27-31.
16. Ankita Sati, Sushil Chandra Sati, Nitin Sati & O. P. Sati (2017) Chemical composition and antimicrobial activity of fatty acid methyl ester of *Quercus leucotrichophora* fruits, *Natural Product Research.* 2017; 31(6), 713-717.
17. National Center for Biotechnology Information. PubChem Database. Linolenic acid, CID=5280934, <https://pubchem.ncbi.nlm.nih.gov/compound/Linolenic-acid> (accessed on May 9, 2020).
18. National Center for Biotechnology Information. PubChem Database. Linoelaidic acid, CID=5282457, <https://pubchem.ncbi.nlm.nih.gov/compound/Linoelaidic-acid> (accessed on May 9, 2020)